

Quantification of Magnetic Domain Disorder and Correlations in Antiferromagnetically Coupled Multilayers by Neutron Reflectometry

Sean Langridge and Jörg Schmalian*

Rutherford Appleton Laboratory, Chilton, Didcot, Oxfordshire OX11 0QX, United Kingdom

C. H. Marrows, D. T. Dekadjevi, and B. J. Hickey

Department of Physics and Astronomy, E. C. Stoner Laboratory, University of Leeds, Leeds LS2 9JT, United Kingdom

(Received 20 May 1999)

The in-plane correlation lengths and angular dispersion of magnetic domains in a transition metal multilayer have been studied using off-specular neutron reflectometry techniques. A theoretical framework considering both structural and magnetic disorder has been developed, quantitatively connecting the observed scattering to the in-plane correlation length and the dispersion of the local magnetization vector about the mean macroscopic direction. The antiferromagnetic domain structure is highly vertically correlated throughout the multilayer. We are easily able to relate the neutron determined magnetic domain dispersion to magnetization and magnetoresistance experiments.

PACS numbers: 75.70.Cn, 75.25.+z, 75.70.Pa

It has become commonplace that magnetic multilayers comprising $3d$ ferromagnetic layers interleaved with non-magnetic spacers exhibit giant magnetoresistance (GMR) for appropriate thicknesses of spacer layer [1]. These are the regimes of the oscillatory interlayer coupling [2] where the ground state is an antiferromagnetic (AF) alignment of neighboring layer magnetizations. The change in resistivity arises from the spin dependent scattering of the conduction electrons which depends not only on the magnetic moment alignment but also on the interfacial disorder [3] and the details of the magnetic domain structure. For example, it is clear that a vertically incoherent magnetic domain structure will have the effect of lowering the GMR by preventing perfect AF alignment in adjacent layers [4]. The determination of the properties of buried layers and interfaces is a long-standing experimental problem in the study of heterostructures such as these multilayers. The investigation of *structurally* rough interfaces is now well established and makes use of diffuse x-ray scattering techniques. The theoretical tools for analyzing various interface morphologies are well advanced [5–8]. Recent advances in x-ray techniques have applied this structural formalism to the study of “magnetically rough” systems [9–15]. Nevertheless, the problem of quantifying magnetic disorder by this method remains difficult, primarily due to the indirect and complicated nature of the spin-photon interaction [16,17]. Using neutron techniques, for which the interaction between the neutron’s dipole moment and the sample magnetization is simple and direct, this problem can be resolved.

In this Letter we report on neutron scattering measurements on magnetically coupled multilayers and the quantitatively determined field dependence of the domain distribution. The large lateral coherence length of the neutron beam, $>30 \mu\text{m}$ [18], ensures that the measurements sample many magnetic domains, often not the case with even advanced synchrotron sources (coherence length

typically $\sim 1 \mu\text{m}$ [19]). Since the neutrons are highly penetrative the measurements also sample the whole multilayer vertically, unlike, for example, the transition metal L_{III} x-ray measurements [20], which sample primarily the uppermost interfaces because of the high x-ray absorption coefficient.

A further complication is that magnetization is a vector quantity and so is able to display a greater variety of different types of disorder than a structural surface, represented mathematically by a scalar function. A uniformly magnetized layer having a structurally rough interface will also have a magnetic surface which deviates from an ideal plane, and is said to possess *magnetic roughness* [21]. On the other hand, a nonuniform distribution of magnetization direction is termed a domain structure and is also a form of magnetic disorder. Both these types of disorder will give rise to off-specular magnetic scatter, and care must be taken to distinguish these experimentally.

Co/Cu multilayers of 50 bilayer repeats, with Cu spacer thicknesses corresponding to both of the first two AF regions of the coupling oscillation [2], were deposited by dc magnetron sputtering at 3 \AA/s in 3 mTorr of Ar. The reflectivity measurements were performed on the time-of-flight polarized neutron reflectometer CRISP at the ISIS facility [22,23]. To maximize the flux the reflectometer was run in the nonpolarized mode with an incident wavelength range of $0.5\text{--}6.5 \text{ \AA}$. An electromagnet at the sample position provides an in-plane reversible field of $\pm 7 \text{ kOe}$. The scattered neutrons are detected by a one-dimensional ^3He detector. The combination of the time-of-flight technique and the multidetector ensure that both the parallel (Q_Z) and perpendicular (Q_X) (to the surface normal) components of the neutron wave-vector transfer (see Fig. 1) are obtained in a single measurement. Typical acquisition times are of the order of 2 h for an entire reciprocal space map, which compares favorably with resonant x-ray techniques [20].

Figure 1(a) shows the observed reciprocal space intensity map for the nominal $[\text{Co}(20 \text{ \AA})/\text{Cu}(20 \text{ \AA})] \times 50$ multilayer at remanence. This Cu thickness corresponds to the second AF peak in the oscillatory exchange coupling. Although we have similar data for other layer thicknesses we concentrate on this sample in this Letter. Three features are apparent in the data: the specularly reflected ridge ($Q_x = 0 \text{ \AA}^{-1}$), the first order nuclear Bragg peak ($Q_z = 0.15 \text{ \AA}^{-1}$), and the $\frac{1}{2}$ order Bragg peak corresponding to the AF periodicity ($Q_z = 0.075 \text{ \AA}^{-1}$). The nuclear Bragg peak indicates that the bilayer thickness is $\sim 42 \text{ \AA}$.

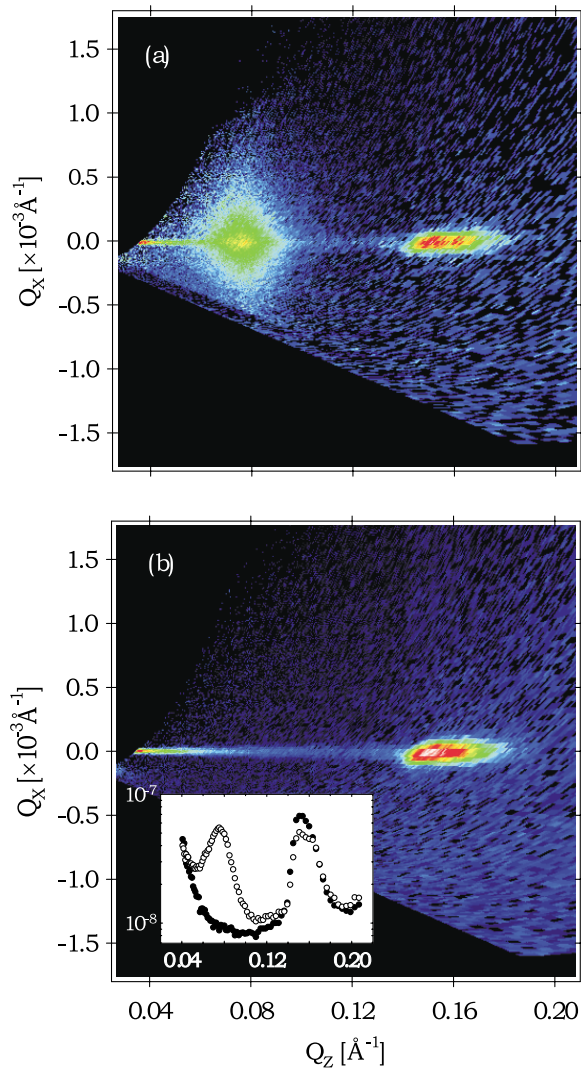


FIG. 1 (color). (a) The observed scattering from the $[\text{Co}(20 \text{ \AA})/\text{Cu}(20 \text{ \AA})] \times 50$ multilayer in zero applied field. The intensity centered at $Q_z = 0.075 \text{ \AA}^{-1}$ corresponds to the AF ordering wave vector and arises purely from the magnetic ordering. The intensity at twice this wave vector is the first order multilayer structural Bragg peak. The dark areas represent the kinematical limits of the measurement. (b) The corresponding measurement in a saturation field of $H = 700 \text{ Oe}$. The nuclear peak appears wider than the specular ridge at low Q_z since the instrumental resolution in Q_x degrades as the reciprocal of the neutron wavelength. The inset shows the specular reflectivity for the low (open symbol) and high (closed symbol) field data.

The narrow width in Q_z (see inset) implies that the AF order is coherent throughout the whole multilayer.

A major conclusion of this paper results from the comparison of the Q_x distribution of the two peaks. The nuclear Bragg peak is sharp but the AF peak, entirely magnetic in origin, is diffuse. The low structural roughness is consistent with the results of conventional x-ray studies of similar samples, where rms roughnesses as low as 1 \AA were found [24]. When at saturation [Fig. 1(b)] the diffuse scatter is very weak over the entire Q_z range in question, and so we associate the diffuse scatter around the magnetic peak in Fig. 1(a) with the existence of AF coupled domains. In contrast, in a study of Fe/Cr multilayers the magnetic diffuse scatter moved from around the AF $\frac{1}{2}$ order peak into *diffuse* scatter around the first order peak on application of a saturating field [25]. Sinha has shown that this is due to the presence of magnetic roughness, not domains, as domain disorder is swept out by a saturating field [26].

The diffuse scattering is strongly peaked in Q_z , giving evidence for the coherent coupling of the magnetic domains vertically through the multilayer. No evidence for diffuse scattering from uncorrelated regions was observed which would be uniformly distributed in Q_z [27]. Applying a saturating field [Fig. 1(b)] destroys the AF correlations resulting in a ferromagnetic alignment of adjacent Co layer moments. Figure 2 details sections in Q_x through the AF Bragg peak as the field is applied. At low fields ($< 100 \text{ Oe}$) the diffuse scatter dominates. As the field is increased to saturation only the specular ridge remains. Equivalent sections through the nuclear Bragg peak reveal no evidence of diffuse scattering at any field.

In order to quantitatively analyze our data a theoretical framework for diffuse magnetic scattering in systems with both structural and magnetic disorder is required. Considering a system where the magnetization profile $\mathbf{m}(\mathbf{r})$ is constrained to lie in the sample plane due to the shape anisotropy, we can write $\mathbf{m}(\mathbf{r}) = M_{\text{Co}}[\cos\phi(\mathbf{r}), \sin\phi(\mathbf{r}), 0]$, with $\phi(\mathbf{r})$ being the local direction of the magnetization, which is of magnitude M_{Co} . Thus, we consider solely directional variations of $\mathbf{m}(\mathbf{r})$ which describe the different orientations of the magnetic domains. We treat $\phi(\mathbf{r})$ as a random variable, characterized by the correlation function $M(|\mathbf{r}|) = \langle \phi(\mathbf{r})\phi(0) \rangle$. $\phi(\mathbf{r})$ plays a role reminiscent of the local height variation in the structural model of Sinha [5], and we parametrize $M(r)$ as

$$M(r) = \sigma_m^2 e^{-(r/\xi_m)}. \quad (1)$$

$\sigma_m = \langle \phi^2 \rangle$ is the width of the angular distribution and therefore characterizes the *magnetic domain disorder*. ξ_m is the lateral correlation length, i.e., a measure of a typical domain size. Structural roughness is included following the formalism of Sinha [5]. We consider the magnetic scattering function within the Born approximation, $S(\mathbf{Q}) \propto \sum_{\alpha\beta} \int d^3\mathbf{r} \langle e^{i\mathbf{Q}\cdot\mathbf{r}} (\delta_{\alpha\beta} - \hat{Q}_\alpha \hat{Q}_\beta) m_\alpha(\mathbf{r}) m_\beta(0) \rangle$, where \hat{Q}_α is a unit vector component of the transferred momentum,

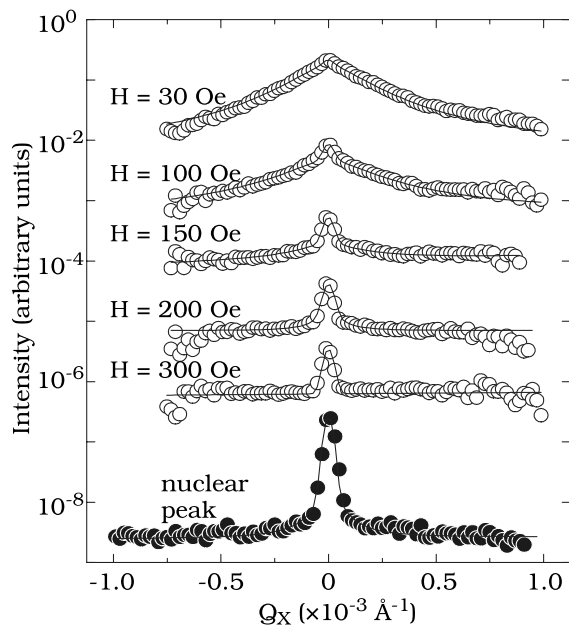


FIG. 2. The diffuse scattering observed at the AF peak ($Q_z = 0.075 \text{ \AA}^{-1}$) as a function of applied field. Each scan is offset for clarity. The lines are fits to the data. The lowest scan (solid symbols) is an equivalent section through the nuclear peak at saturation ($Q_z = 0.15 \text{ \AA}^{-1}$), the width of which is independent of field.

Q. Performing the average with respect to the different domain orientations by assuming a Gaussian distribution for $\phi(\mathbf{r})$, we find in addition to the specular scattering, $S_{\text{spec}}(\mathbf{Q}) = 4\pi^2 D \delta(\mathbf{Q}_{\parallel})$, the diffusive scattering function

$$S_{\text{diff}}(\mathbf{Q}) = D \int d^2\mathbf{r} e^{i\mathbf{Q}_{\parallel}\cdot\mathbf{r}} [s + m + sm], \quad (2)$$

where the terms in square brackets correspond to three different diffuse scatter contributions, arising from structural inhomogeneities, magnetic inhomogeneities, and the interference between them. The joint Debye-Waller factor, D , is expressed as $m_0^2 e^{-(Q_z^2 \sigma_s^2 + \sigma_m^2)}$; m_0 is the antiferromagnetic order parameter, discussed below. The amplitudes of the structural and magnetic inhomogeneities are given by $\sigma_s^2 = C(0)$ and $\sigma_m^2 = M(0)$, with the usual structural correlation function $C(r) = \sigma_s^2 e^{-(r/\xi_s)}$. \mathbf{Q}_{\parallel} is the in-plane component of \mathbf{Q} .

The terms in square brackets in (2) correspond to the three diffuse scatter contributions, with the structural and magnetic parts expressed as

$$s = e^{[Q_z^2 C(r)]}, \quad (3)$$

$$m = (1 - \hat{Q}_x^2) [\sinh(M(\mathbf{r}))] + (1 - \hat{Q}_y^2) [\cosh(M(\mathbf{r})) - 1]. \quad (4)$$

The first of these three diffuse scattering terms is entirely equivalent to that derived by Sinha. The second corresponds to domain distributions, while the final cross term contains the magnetic roughness. The use of this formula allows us to quantify the diffuse scatter due to a domain

distribution, as the neutron spin-magnetization interaction is explicitly included. This was not possible in previous work [25,28,29], where straightforward adaptations of structural models [27,30] were used. In our experimental geometry the detector aperture is set up such that the neutron intensity is integrated out over Q_y , which is parallel to the applied field. Finally, when evaluated at the AF ordering vector, it holds that $m_0 \propto \sin(\theta/2)$, where θ is the angle between Co moments in adjacent layers. In the kinematic picture, the intensity of the $\frac{1}{2}$ order Bragg peak is proportional to m_0^2 . We remark in passing that, within the Gaussian approximation, we treat the angle $\phi(\mathbf{r})$, normally restricted to between $\pm\pi$, as an unrestricted variable. Therefore, the model will only approximately describe a system with equally distributed angles.

The results of numerically convoluting the specular and diffuse [Eq. (2)] contributions with the instrumental resolution function and of performing a least-squares fit to the data are shown in Fig. 2 as the solid lines. To extract the structural—and hence implicitly the magnetic—correlated roughness parameter we have fitted the specular reflectivity at saturation, where the sample is in a single domain state, i.e., $\sigma_m = 0$ and $\xi_m = \infty$. The structural roughness $\sigma_s = 3 \pm 1 \text{ \AA}$ extracted is consistent with previous x-ray results [31]. At this level no diffuse scattering from the structural roughness is observable in our experimental data—the width of the specular ridge is determined by instrumental resolution. This structural parameter has been used in all the fits at lower fields to ensure we are varying only the domain structure within our model. We have found that the domain disorder is by far the main contribution to the diffuse scatter at all fields below total saturation.

In Fig. 3 we show various magnetic quantities for our sample as a function of applied field. Panels (a) and (b) display the magnetization loop as measured by magneto-optic Kerr effect (MOKE) and the normalized change in resistivity (GMR), respectively. The large GMR indicates a high degree of AF alignment around the coercive field. The final three panels indicate quantities derived from our fits to the neutron diffuse scatter. For fields close to remanence the Co layers have a global antiparallel alignment (c) with a wide distribution of domain directions (d) and a characteristic domain size of $\sim 1 \mu\text{m}$ (e). As the field is applied three effects occur in order, but with considerable overlap: the antiparallel alignment across the nonmagnetic spacer is diminished, the orientational domain distribution within a given layer focuses around the applied field direction, and at field higher than the coercivity the domains enlarge to $\sim 7 \mu\text{m}$. Above $\sim 200 \text{ Oe}$ there still remains a substantial domain distribution, although the orientation of adjacent layers is nearly ferromagnetic ($m_0 \rightarrow 0$). At these fields the diffuse scattering approaches the experimental background (primarily from incoherent scattering) and represents the limits of the current measurements. For this reason we cannot measure values of σ_m close to zero as saturation is approached. The data clearly show the

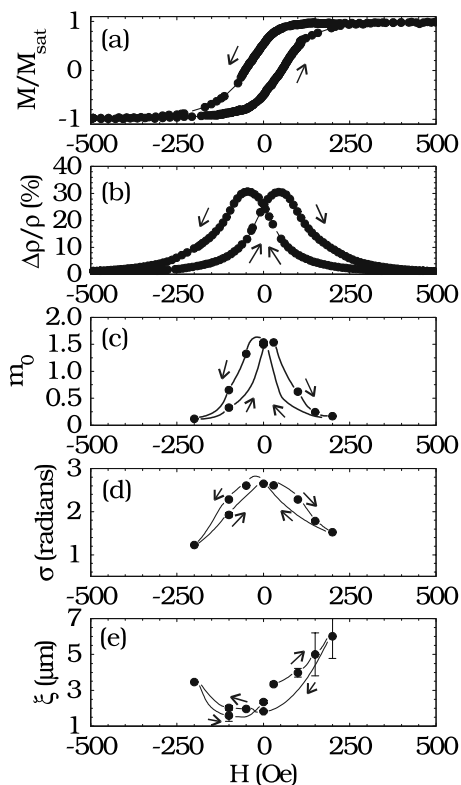


FIG. 3. (a) The room temperature MOKE magnetization loop for the $[\text{Co}(20 \text{ \AA})/\text{Cu}(20 \text{ \AA})] \times 50$ sample. (b) The magnetoresistance. Panels (c), (d), and (e) represent the parameters described in the text. The lines are simply guides to the eye.

hysteresis in moving around the loop. The fact that all quantities in Fig. 3 follow this hysteresis loop reveals the close correlation between the GMR effect and the magnetic domain correlations. The decrease of the angle θ between the magnetization in neighboring layers causes not only the expected decrease of the GMR but is accompanied by a narrowing domain spread, and larger domains. The observed rise in domain size from ~ 1 to $7 \mu\text{m}$ is typical of such systems [32]. We have observed qualitatively similar effects around the nuclear/ferromagnetic Bragg peak for an equivalent ferromagnetically coupled system.

Our results can be compared with recent work on a weakly coupled system (Ref. [28]). The reduction in the GMR from the as-prepared state to the coercive state was shown to be a loss of vertical coherence of the AF alignment. The more strongly coupled samples studied here clearly show highly correlated domains at the coercive field.

To summarize, we have developed a theoretical framework allowing quantification of the magnetic domain structure in an AF coupled multilayer using diffuse magnetic neutron scattering. The systematic study of the field dependence of the diffuse scattering reveals a close rela-

tionship between domain disorder, domain size, interlayer coupling, and the GMR effect itself.

The authors gratefully acknowledge fruitful discussions with M. Sferazza, J.R.P. Webster, J. Penfold, S.W. Lovesey, A.I. Goldman, and S.K. Sinha. C.H.M. thanks the Royal Commission for the Exhibition of 1851 for financial support. We are grateful to the Rutherford Appleton Laboratory for the provision of ISIS beam time.

*Present address: Department of Physics, Iowa State University, and Ames Laboratory, Ames, IA 50011.

- [1] M.N. Baibach *et al.*, Phys. Rev. Lett. **61**, 2472 (1988).
- [2] S.S.P. Parkin, N. More, and K.P. Roche, Phys. Rev. Lett. **64**, 2304 (1990); S.S.P. Parkin, R. Bhadra, and K.P. Roche, Phys. Rev. Lett. **66**, 2152 (1991).
- [3] P. Zahn *et al.*, Phys. Rev. Lett. **80**, 4309 (1998).
- [4] H. Holloway and D.J. Kubinski, J. Appl. Phys. **83**, 2705 (1998).
- [5] S.K. Sinha *et al.*, Phys. Rev. B **38**, 2297 (1988).
- [6] S.K. Sinha *et al.*, Physica (Amsterdam) **198B**, 72 (1994).
- [7] V. Holý *et al.*, Phys. Rev. B **49**, 10 668 (1994).
- [8] R. Pynn, Phys. Rev. B **45**, 602 (1992).
- [9] C.T. Chen *et al.*, Phys. Rev. B **48**, 642 (1993).
- [10] J.W. Freeland *et al.*, J. Appl. Phys. **83**, 6290 (1998).
- [11] Y.U. Idzerda *et al.*, Phys. Rev. Lett. **82**, 1562 (1999).
- [12] J.F. MacKay *et al.*, Phys. Rev. Lett. **77**, 3925 (1996).
- [13] C. Kao *et al.*, Phys. Rev. Lett. **65**, 373 (1990).
- [14] P. Fischer *et al.*, J. Phys. D **31**, 645 (1998).
- [15] V. Chakarian *et al.*, Appl. Phys. Lett. **66**, 3368 (1995).
- [16] D. Gibbs *et al.*, Phys. Rev. Lett. **61**, 1241 (1988).
- [17] J.P. Hannon *et al.*, Phys. Rev. Lett. **61**, 1245 (1988).
- [18] J.F. Ankner and G.P. Felcher, J. Magn. Magn. Mater. **200**, 751 (1999).
- [19] T.P.A. Hase (private communication).
- [20] T.P.A. Hase, Ph.D. thesis, University of Durham, 1998.
- [21] R. Osgood III *et al.*, J. Magn. Magn. Mater. **199**, 698 (1999).
- [22] R. Felici *et al.*, Appl. Phys. A **45**, 169 (1988).
- [23] <http://www.isis.rl.ac.uk/largescale/crisp/CRISP.htm>
- [24] C.H. Marrows *et al.*, J. Phys. Condens. Matter. **11**, 81 (1999).
- [25] M. Takeda *et al.*, Physica (Amsterdam) **248B**, 14 (1998).
- [26] S.K. Sinha, Mater. Res. Soc. Symp. Proc. **376**, 175 (1995).
- [27] D.E. Savage *et al.*, J. Appl. Phys. **69**, 1411 (1991).
- [28] J.A. Borchers *et al.*, Phys. Rev. Lett. **82**, 2796 (1999).
- [29] W. Hahn *et al.*, J. Appl. Phys. **75**, 3564 (1994).
- [30] R.W. James, *The Optical Principles of Diffraction of X-Rays* (Cornell University Press, Ithaca, 1962).
- [31] T.P.A. Hase *et al.*, Phys. Rev. B **61**, R3792 (2000); ξ_s cannot be determined reliably from the neutron data as the diffuse scatter is so weak at saturation—it was found to be $\sim 250 \text{ \AA}$ by x rays in the cited work.
- [32] L.J. Heyderman, J.N. Chapman, and S.S.P. Parkin, J. Phys. D **27**, 881 (1994).